CHAPTER

# FIVE

# INTRODUCTION TO STRAIN MEASUREMENTS

## 5.1 DEFINITION OF STRAIN AND ITS RELATION TO EXPERIMENTAL DETERMINATIONS

A state of strain may be characterized by its six cartesian strain components or, equally well, by its three principal strain components with the three associated principal directions. The six cartesian components of strain are defined in terms of the displacement field by the following set of equations when the strains are small (normally the case for elastic analyses):

$$\epsilon_{xx} = \frac{\partial u}{\partial x} \qquad \epsilon_{yy} = \frac{\partial v}{\partial y} \qquad \epsilon_{zz} = \frac{\partial w}{\partial z}$$

$$\gamma_{xy} = \frac{\partial v}{\partial x} + \frac{\partial u}{\partial y} \qquad \gamma_{yz} = \frac{\partial w}{\partial y} + \frac{\partial v}{\partial z} \qquad \gamma_{zx} = \frac{\partial u}{\partial z} + \frac{\partial w}{\partial x} \tag{2.4}$$

The $\epsilon$ components are normal strains, and $\epsilon_{xx}$, for instance, is defined as the change in length of a line segment parallel to the $x$ axis divided by its original length. The $\gamma$ components are shearing strains, and $\gamma_{xy}$, for instance, is defined as the change in the right angle formed by line segments parallel to the $x$ and $y$ axes.

For the most part, strain-gage applications are confined to the free surfaces of a body. The two-dimensional state of stress existing on this surface can be expressed in terms of three cartesian strains $\epsilon_{xx}$, $\epsilon_{yy}$, and $\gamma_{xy}$. Thus, if the two displacements $u$ and $v$ can be established over the surface of the body, the strains can be determined directly from Eqs. (2.4). In certain isolated cases, the most

appropriate approach for the determination of the stress and strain field is the determination of the displacement field. As an example, consider the very simple problem of a transversely loaded beam. The deflections of the beam $w(x)$ along its longitudinal axis can be accurately determined with relatively simple experimental techniques. The strains and stresses are related to the deflection $w(x)$ of the beam by

$$\epsilon_{xx} = \frac{z}{\rho} = z\frac{d^2w}{dx^2} \qquad \sigma_{xx} = E\epsilon_{xx} = Ez\frac{d^2w}{dx^2} \tag{5.1}$$

where $\rho$ is the radius of curvature of the beam and $z$ is the distance from the neutral axis of the beam to the point of interest

Measurement of the transverse displacements of plates can also be accomplished with relative ease, and stresses and strains computed by employing equations similar to (5.1). In the case of a more general body, however, the displacement field cannot readily be measured. Also, the conversion from displacements to strains requires a determination (by differentiation) of the gradients of experimentally determined displacements at many points on the surface of the specimen. Since the displacements are often difficult to obtain and the differentiation process is subject to large errors, it is advisible to employ a strain gage of one form or another to measure the surface strains directly.

Examination of Eqs. (2.4) shows that the strains $\epsilon_{xx}$, $\epsilon_{yy}$, and $\gamma_{xy}$ are really the slopes of the displacement surfaces $u$ and $v$. Moreover, these strains are not, in general, uniform; instead, they vary from point to point. The slopes of the displacement surfaces cannot be established unless the in-plane displacements $u$ and $v$ can be accurately established. Since the in-plane displacements are often exceedingly small in comparison with the transverse (out-of-plane) displacements mentioned previously, their direct measurement over the entire surface of a body is exceedingly difficult. To circumvent this difficulty, one displacement component is usually measured over a small portion of the body along a short line segment, as illustrated in Fig. 5.1. This displacement measurement is converted to strain by the relationship

$$\epsilon_{xx} = \frac{l_x - l_0}{l_0} = \frac{\Delta u}{\Delta x} \tag{5.2}$$

where $\Delta u = l_x - l_0$ is the displacement in the $x$ direction over the length of the line segment $l_0 = \Delta x$. Strain measured in this manner is not exact since the determination is made over some finite length $l_0$ and not at a point, as the definition for strain $\epsilon$ requires. The error involved in this approach depends upon the strain gradient and the length of the line segment $l_0$. If the strain determination is considered to represent the strain which occurs at the center of the line segment $l_0$, that is, point $x_1$, the error involved for various strain gradients is

Case 1, strain constant: $\epsilon_{xx} = k_1$ (no error is induced)
Case 2, strain linear: $\epsilon_{xx} = k_1 x + k_2$ (no error is induced)
Case 3, strain quadratic: $\epsilon_{xx} = k_1 x^2 + k_2 x + k_3$

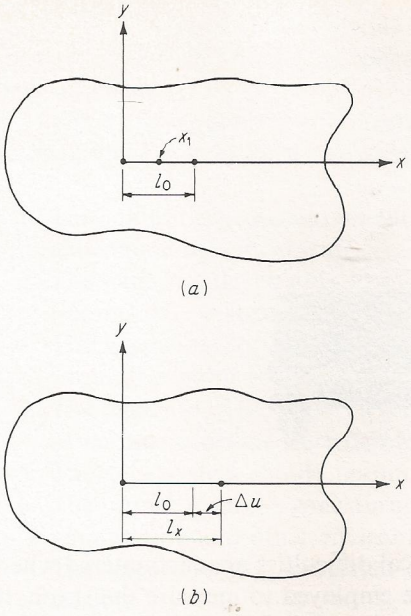


**Figure 5.1** Strain measurement over a short line segment of length $l_0$: (*a*) before deformation; (*b*) after deformation.

In case 3, an error is involved since the strain at the midpoint $x_1$ is not equal to the average strain over the gage length $l_0$. The average strain over the gage length $l_0$ can be computed as

$$\epsilon_{av} = \frac{\int_0^{l_0} (k_1 x^2 + k_2 x + k_3)\, dx}{l_0} = \frac{k_1 l_0^2}{3} + \frac{k_2 l_0}{2} + k_3 \qquad (a)$$

and the strain at the midpoint $x_1 = l_0/2$ is given by

$$\epsilon_{xx}\Big|_{x_1} = \frac{k_1 l_0^2}{4} + \frac{k_2 l_0}{2} + k_3 \qquad (b)$$

The difference between the average and midpoint strains represents the error involved and is given by

$$\text{Error} = \frac{k_1 l_0^2}{12} \qquad (5.3)$$

In this example the error involved depends upon the values of $k_1$ and $l_0$. If the gradient is sharp, the value of $k_1$ will be significant and the error induced will be large unless $l_0$ is reduced to an absolute minimum. Other examples corresponding to cubic and quartic strain distributions can also be analyzed; however, the fact that an error is induced is established by considering any strain distribution other than a linear one.

In view of the error introduced by the length of the line segment in certain strain fields, great effort has been expended in reducing the gage length $l_0$. Two

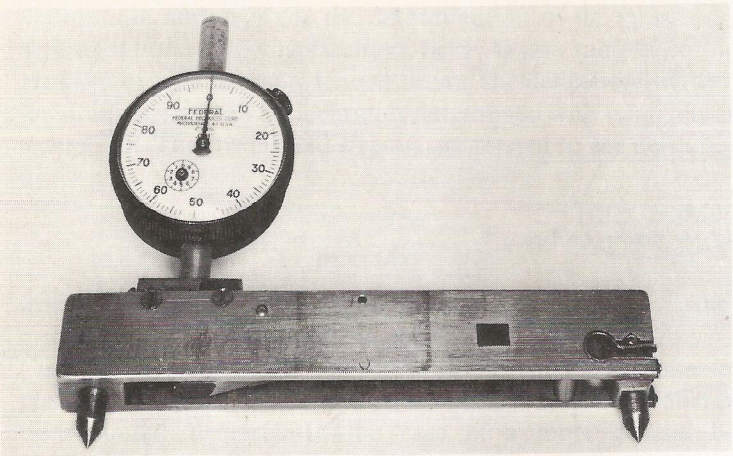

**Figure 5.2** Berry-type strain gage.

factors complicate these efforts. (1) Mechanical difficulties are encountered when $l_0$ is reduced. Regardless of the type of gage employed to measure the strain, it must have a certain finite size and a certain number of parts. As the size is reduced, the parts become smaller and the dimensional tolerances required on each become prohibitive. (2) The strain to be measured is a very small quantity. Suppose, for example, that strain determinations are to be made with an accuracy of $\pm 1$ $\mu$in/in ($\mu$m/m) over a gage length of 0.1 in (2.5 mm). The strain gage must measure the corresponding displacement to an accuracy of $\pm 1 \times 10^{-6} \times 0.1 = \pm 1 \times 10^{-7}$ in (2.5 nm) or one-ten-millionth of an inch. These size and accuracy requirements place heavy demands on the talents of investigators in the area of strain-gage development.

The smallest gage developed and sold commercially to date is the electrical-resistance type. This gage is prepared from an ultrathin alloy foil which is photoetched to produce the intricate grid construction with a gage length of only 0.008 in (0.2 mm). On the other hand, mechanical strain gages are still employed in civil engineering structural applications where the gage length $l_0 = 8$ in or 200 mm (Berry strain gage). These Berry gages are rugged, simple to use, and sufficiently accurate in structural applications where the strain distribution is approximately linear over the 8-in (200-mm) gage length. A Berry-type strain gage is shown in Fig. 5.2.

## 5.2 PROPERTIES OF STRAIN-GAGE SYSTEMS

Historically, the development of strain gages has followed many different paths, and gages have been developed which are based on mechanical, optical, electrical, acoustical, and pneumatic principles. No single gage system, regardless of the principle upon which it is based, has all the properties required of an optimum

gage. Thus a need exists for a wide variety of gaging systems to meet the requirements of a wide range of different engineering problems involving strain measurement.

Some of the optimum characteristics commonly used to judge the adequacy of a strain-gage system for a particular application are the following:

1. The calibration constant for the gage should be stable; it should not vary with either time or temperature.
2. The gage should be able to measure strains with an accuracy of $\pm 1$ $\mu$in/in ($\mu$m/m) over a strain range of 10 percent.
3. The gage size, i.e., the gage length $l_0$ and width $w_0$, should be small so that strain at a point is adequately approximated.
4. The response of the gage, largely controlled by its inertia, should be sufficient to permit recording of dynamic strains.
5. The gage system should permit on-location or remote readout.
6. The output from the gage during the readout period should be independent of temperature and other environmental parameters.
7. The gage and the associated auxiliary equipment should be economically feasible.
8. The gage system should not involve overcomplex installation and operational techniques.
9. The gage should exhibit a linear response to strain.
10. The gage should be suitable for use as the sensing element in other transducer systems where an unknown quantity such as pressure is measured in terms of strain.

No single strain-gage system satisfies all these optimum characteristics. The strain-gage system for a particular application can be selected after proper consideration is given to each of these characteristics in terms of the requirements of the measurement to be made. Over the last 50 years a large number of systems, with wide variations in design, have been conceived, developed, and marketed; however, each system has four basic characteristics which deserve additional consideration. These are the gage length $l_0$, the gage sensitivity, the range of strain, and the accuracy or precision of the readout.

Strains cannot be measured at a point with any type of gage, and, as a consequence, nonlinear strain fields cannot be measured without some degree of error being introduced. In these cases, the error will definitely depend on the gage length $l_0$ in the manner described in Sec. 5.1 and may also depend on the gage width $w_0$. The gage size for a mechanical strain gage is characterized by the distance between the two knife-edges in contact with the specimen (the gage length $l_0$) and by the width of the movable knife-edge (the gage width $w_0$). The gage length of the metal-film resistance strain gage is determined by the length of the strain portion of the grid, and the width $w_0$ is determined by the width of the grid. In selecting a gage for a given application, gage length is one of the most important considerations.

A second basic characteristic of a strain gage is its sensitivity. Sensitivity is the smallest value of strain which can be read on the scale associated with the strain gage. The term sensitivity should not be mistaken for accuracy or precision, since very large values of magnification can be designed into a gage to increase its sensitivity; but friction, wear, and deflection introduce large errors which limit the accuracy. In certain applications gages can be employed with sensitivities of less than 1 $\mu$in/in ($\mu$m/m) if proper procedures are established. In other applications, where sensitivity is not important, 50 to 100 $\mu$in/in ($\mu$m/m) is often quite sufficient. The choice of a gage is dependent upon the degree of sensitivity required, and quite often the selection of a gage with a very high sensitivity when it is not really necessary needlessly increases the complexity of the measuring method.

A third basic characteristic of a strain gage is its range. Range represents the maximum strain which can be recorded without resetting or replacing the strain gage. The range and sensitivity are interrelated since very sensitive gages respond to small strains with appreciable indicator deflections and the range is usually limited to the full-scale deflection of the indicator. Often it is necessary to compromise between the range and sensitivity characteristics of a gage to obtain reasonable performance for both these categories.

The final basic consideration is the accuracy or precision. As was previously pointed out, sensitivity does not ensure accuracy. Usually the very sensitive instruments are quite prone to errors unless they are employed with the utmost care. In a mechanical strain gage, inaccuracies may result from lost motion such as backlash in a gear train, friction, temperature changes, wear in the mechanism, slippage, or flexure or deflection of the components. On all strain gages there is a readout error whether the gage is manually recorded or the output is read on a digital printer.

## 5.3 TYPES OF STRAIN GAGE

The problem encountered in measuring strain is to determine the motion between two points some distance $l_0$ apart. The physical principles which have been employed to accomplish this task are very numerous, and a complete survey will not be attempted; however, a few of the more applicable methods will be covered briefly. The principles employed in strain-gage construction can be used as the basis for classifying the gages into the following four groups:

1. Mechanical
2. Optical
3. Electrical
4. Acoustical

## A. Mechanical Strain Gages [1–5]

The mechanical gage to be considered here is the Huggenberger tensometer, which is the most popular and one of the most accurate mechanical strain gages in use today. The gage shown in Figs. 5.3 and 5.4 is based entirely on mechanical principles. The displacement of the movable knife-edge is multiplied by a set of compound levers until a magnification of displacement up to 2000 is obtained.

The operation of the Huggenberger tensometer is illustrated in Fig. 5.4. The frame $C$ supports the two knife-edges $A$ and $B$ as well as the entire lever system and the indicating scale $Z$. The knife edge $A$ is fixed rigidly to the frame $C$, whereas the knife-edge $B$ rotates about a fixed point on the frame a distance $v_1$ from the specimen. This knife-edge thus serves as the first lever in the system, and since it is also an integral part of the arm $H$, the displacement $\Delta l$ is transmitted to point $M$, where it has been magnified to a distance $\Delta s$. The value of $\Delta s$ is given by the simple lever rule as

$$\Delta s = \frac{v_2}{v_1} \Delta l$$

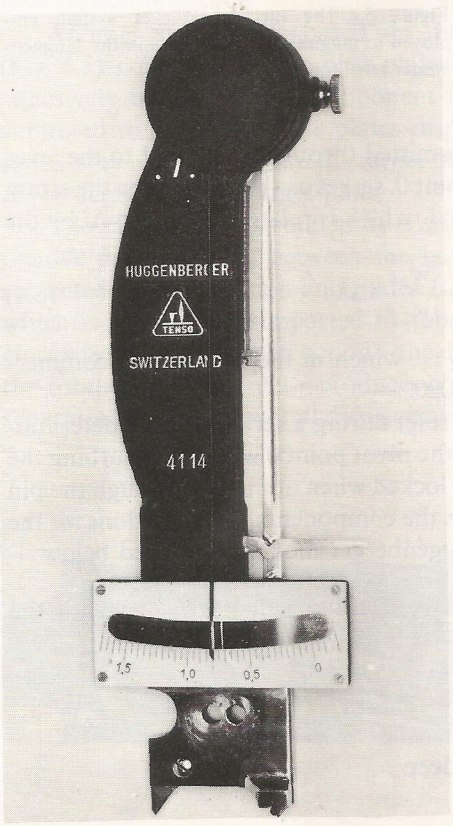


**Figure 5.3** The Huggenberger tensometer.

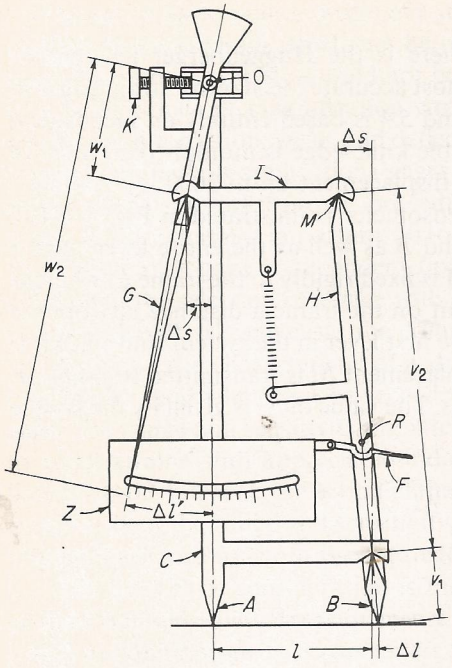


**Figure 5.4** The mechanical-lever system employed to magnify displacements in the Huggenberger tensometer.

The motion at point $M$, that is, $\Delta s$, is transmitted through the yoke $I$ to the lever $G$. The lever $G$, which rotates about the point 0, serves as the pointer for the strain gage. The pointer moves over a distance $\Delta l'$, which is related to $\Delta s$ and $\Delta l$ by the expression

$$\Delta l' = \frac{w_2}{w_1}\Delta s = \frac{w_2 v_2}{w_1 v_1}\Delta l \tag{5.4}$$

The magnification factor is thus $w_2 v_2 / w_1 v_1$, which in the five models commercially available ranges between 300 and 2000.

The Huggenberger tensometer can be reset during a series of strain determinations by rotating the screw which moves the pivot point 0 without disturbing the rest of the linkage system. The gage can be locked when not in use through the pin $R$ and lever $F$ to avoid unnecessary wear on the components. Specifications for the type $A$ gage, one of the most popular Huggenberger models, are listed below:

Multiplication approximately 1200 (exact calibration value provided with the instrument)
Gage length: 1 in convertible to $\frac{1}{2}$ in
Scale 38 divisions: 0.05 in each division
Strain range: 0.004 in without resetting
Dimensions: $6\frac{1}{2}$ in high, $2\frac{1}{16}$ in wide, $\frac{5}{8}$ in deep
Weight: $2\frac{1}{2}$ oz
Accuracy: $\pm 10$ $\mu$in/in

The gage is mounted by clamps, springs, or screw pressure applied to the frame $C$ in sufficient magnitude to set the knife-edges into the specimen. This is perhaps the most objectionable feature in the application of the Huggenberger gage. The knife-edges must be set well enough to avoid slippage of either knife-edge yet not tight enough to damage the gage or the specimen. This clamping process is further complicated by the great height of the gage, which makes it quite unstable in mounting. However, when proper fixturing is available and the operator has developed some skill, the mounting procedure can be accomplished in a reasonable time.

The instrument is definitely limited to static measurements of strain since its size and inertia rule out any chance of a reasonable frequency response, which is required in dynamic applications. Care should also be exercised in keeping the instrument in calibration. The knife-edge $B$ has a tendency to wear, thus shortening the distance $v_1$ and changing the multiplication factor.

In comparison with other mechanical gages the Huggenberger and the Johansson Mikrokator are the most accurate, sensitive, and reliable of the entire line. However, since the advent of the electrical-resistance strain gage, the general use of mechanical strain gages has declined appreciably until today they are used only in special applications.

Another strain gage based on mechanical principles is the scratch gage (Fig. 5.5), consisting of two base plates $L$ and $S$, which can be welded, bolted, or adhesively bonded to the component being evaluated. When the component is subjected to loads, the base plates displace relative to each other and cause the stylus $D$ to move relative to the target plate $T$. The stylus records the displacement $\Delta u$ by scratching the target plate.

The target plate is rotated by a wire drive system, which is activated by the relative displacements between the base plates. For instance, when the gage is subjected to compression and plates $L$ and $S$ are brought closer together, wire $B$, which is guided and supported by tube $BT$, causes the target to rotate counterclockwise. This combined action—the direct movement of the stylus together with the rotation of the target—produces a slanted line on the target plate and effects separation of the individual displacements associated with different levels of load.

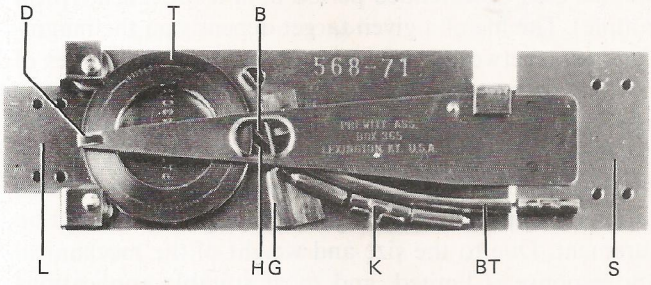


**Figure 5.5** The scratch strain-gage system. (*Prewitt Associates.*)

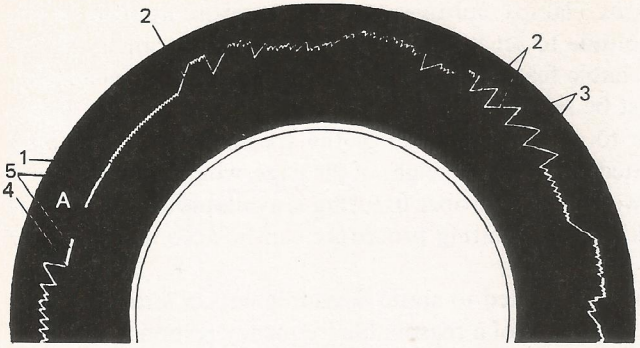


1. Beginning of recording.
2. Compression movement, target rotates.
3. Tension movement, target stationary.
4. End of self-recorder data.
5. Base line arcs.

**Figure 5.6** Enlargement of a target ring with a scratch record. (*Prewitt Associates.*)

An enlargement of a typical scratch record on a target plate is shown in Fig. 5.6.

The target plates are removed from the gage after completion of a test, and the scratch patterns are analyzed with an optical comparator or with a special microscope designed and calibrated for use with the target plates. The width of a scratch on a target plate is approximately 0.0005 in (0.0125 mm) and a movement between plates of 0.004 in (0.10 mm) can be distinguished and measured with reasonable accuracy.

The sensitivity and accuracy of a strain measurement depends upon the gage length and the gradient of the strain field. Gages are available in sizes from 3 to 100 in (75 to 2500 mm); thus, precision measurements (sensitivity between 50 and 100 $\mu$in/in or $\mu$m/m) can be made if the strain field is either constant or linear so that the longer gage lengths can be employed. With shorter gage lengths the sensitivity is significantly reduced.

The target rotates a small amount with each cycle of strain above some minimum threshold level; thus, continuous records of strain cycles above the threshold value can be obtained over an extended period of time (during a typical flight of an aircraft for example). The life of a given target depends on the magnitudes of the relative displacement between base plates; however, 1000 cycles of strain above the threshold value can be used as a rough guide for the life. Since the target plates can be changed, the life of a gage installation can be extended by periodic replacement of the plates.

The gages have a limited capability for the measurement of dynamic strains and can withstand accelerations of approximately $33g$ without significant effect on the accuracy of the measurement. Due to the size and weight of the mechanical components, the frequency response is limited, and most suitable applications involve measurement of quasi-static strains.

## B. Optical Strain Gages [6–10]

In the first edition of this text, the Tuckerman optical strain gage, marketed by the American Instrument Company, was described. This gage is similar in some ways to the Huggenberger type of mechanical gage in that it incorporates knife-edge attachment to the specimen. The chief difference between the two gages is in the lever system, where the optical gage substitutes light rays for the mechanical levers. This substitution decreases the size and inertia of the device appreciably and permits the optical gage to be employed at low frequencies in dynamic applications. Since 1965, considerable research effort has been devoted to the area of optical methods of experimental stress analysis. The availability of gas and ruby lasers as monochromatic, collimated, and coherent light sources has led to several new developments in strain gages. Two of these developments—the diffraction strain gage and the interferometric strain gage—are described to indicate the capabilities of optical gages which use coherent light.

The diffraction strain gage is quite simple in construction; it consists of two blades that are bonded or welded to the component, as illustrated in Fig. 5.7. The two blades are separated by a distance $b$ to form a narrow aperture and are fixed to the specimen along the edges (see Fig. 5.7) to give a gage length $l$. A beam of collimated monochromatic light from a helium-neon laser is directed onto the aperture to produce a diffraction pattern that can be observed as a line of dots on a screen a distance $R$ from the aperture. An example of a diffraction pattern is illustrated in Fig. 5.8.

When the distance $R$ to the screen is very large compared with the aperture width $b$, the distribution of the intensity $I$ of light in the diffraction pattern (see Sec. 11.5) is

$$I = A_0^2 \frac{\sin^2 \beta}{\beta^2} \tag{5.5}$$

where $A_0$ is the amplitude of the light on the centerline of the pattern ($\theta = 0$) and

$$\beta = \frac{\pi b}{\lambda} \sin \theta \tag{5.6}$$

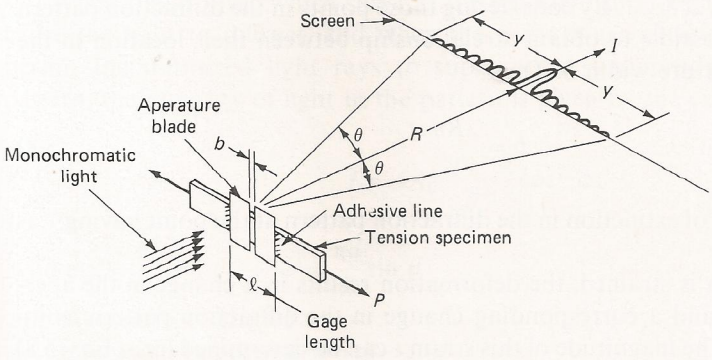


**Figure 5.7** Arrangement of the diffraction-type strain gage. (*After T. R. Pryor and W. P. T. North.*)

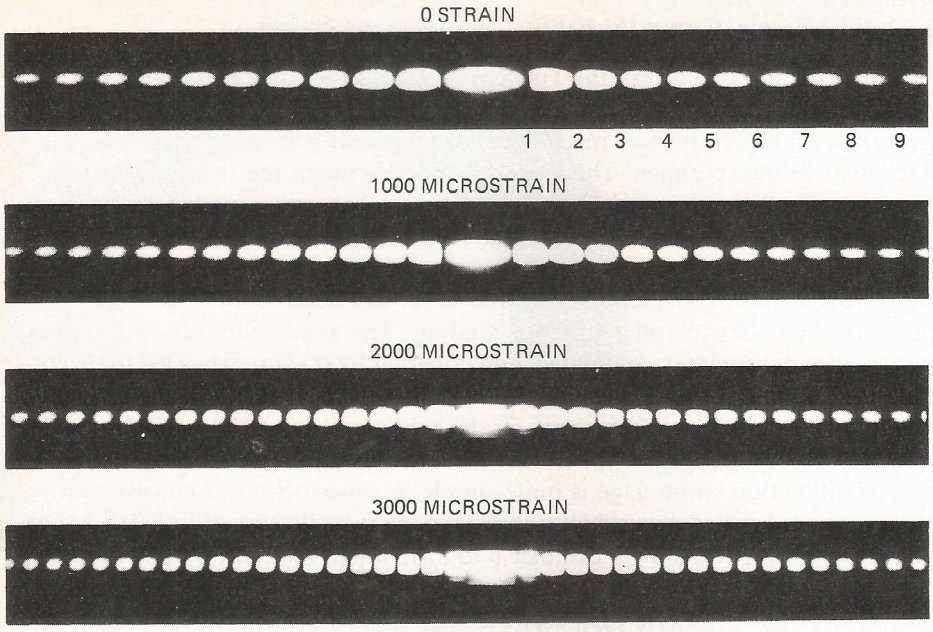


**Figure 5.8** Diffractograms showing changes in the diffraction pattern with increasing strain. (*T. R. Pryor and W. P. T. North.*)

where $\theta$ is defined in Fig. 5.7 and $\lambda$ is the wavelength of the light. If the analysis of the diffraction pattern is limited to short distances $y$ from the centerline of the system, sin $\theta$ is small enough to be represented by $y/R$ and Eq. (5.6) becomes

$$\beta = \frac{\pi b}{\lambda} \frac{y}{R} \tag{5.7}$$

The intensity $I$ vanishes according to Eq. (5.5) when $\sin \beta = 0$ or when $\beta = n\pi$, where $n = 1, 2, 3, \ldots$. By considering those points in the diffraction pattern where $I = 0$, it is possible to obtain a relationship between their location in the pattern and the aperture width $b$. Thus

$$b = \frac{\lambda R n}{y} \tag{5.8}$$

where $n$ is the order of extinction in the diffraction pattern at the point having $y$ as its position.

As the specimen is strained, the deformation results in a change in the aperture width $\Delta b = \epsilon l$ and a corresponding change in the diffraction pattern as indicated in Fig. 5.7. The magnitude of this strain $\epsilon$ can be determined from Eq. (5.8) and measurements from the two diffraction patterns. As an example, consider the

diffraction pattern after deformation, where

$$b + \Delta b = \frac{\lambda R n^*}{y_1} \qquad (a)$$

and the diffraction pattern before deformation, where

$$b = \frac{\lambda R n^*}{y_0} \qquad (b)$$

Subtracting Eq. (*b*) from Eq. (*a*) and simplifying gives the average strain $\epsilon$ over the gage length $l$ as

$$\epsilon = \frac{\Delta b}{l} = \frac{\lambda R n^*}{l} \frac{y_0 - y_1}{y_0 y_1} \qquad (5.9)$$

In practice, the order of extinction $n^*$ is selected as high as possible consistent with the optical quality of the diffraction pattern. When the higher orders of extinction are used, the distance $y$ can be measured with sufficient accuracy with calipers and an engineering scale and elaborate measuring devices can be avoided.

The diffraction strain gage is extremely simple to install and use provided the component can be observed during the test. The method has many advantages for strain measurement at high temperatures since it is automatically temperature-compensated if the blades are constructed of the same material as the specimen.

A second optical method of strain measurement utilizes the interference patterns produced when coherent, monochromatic light from a source such as a helium-neon laser is reflected from two shallow V-grooves ruled on a highly polished portion of the specimen surface. The V-grooves are usually cut with a diamond to a depth of approximately 0.000040 in (0.001 mm) and are spaced approximately 0.005 in (0.125 mm) apart. An interference pattern from a pair of grooves having this depth and spacing and a groove angle of 110° is shown in Fig. 5.9.

When the grooves which serve as the reflective surfaces are small enough to cause the light to diffract, and when the grooves are close enough together to permit the diffracted light rays to superimpose and produce an interference pattern, the intensity of light in the pattern is given by the expression

$$I = 4A_0^2 \frac{\sin^2 \beta}{\beta^2} \cos^2 \phi \qquad (5.10)$$

where $\beta = \dfrac{\pi b}{\lambda} \sin \theta \qquad \phi = \dfrac{\pi d}{\lambda} \sin \theta$

and $b$ = width of groove

$d$ = width between grooves

$\theta$ = angle from central maximum, as previously defined

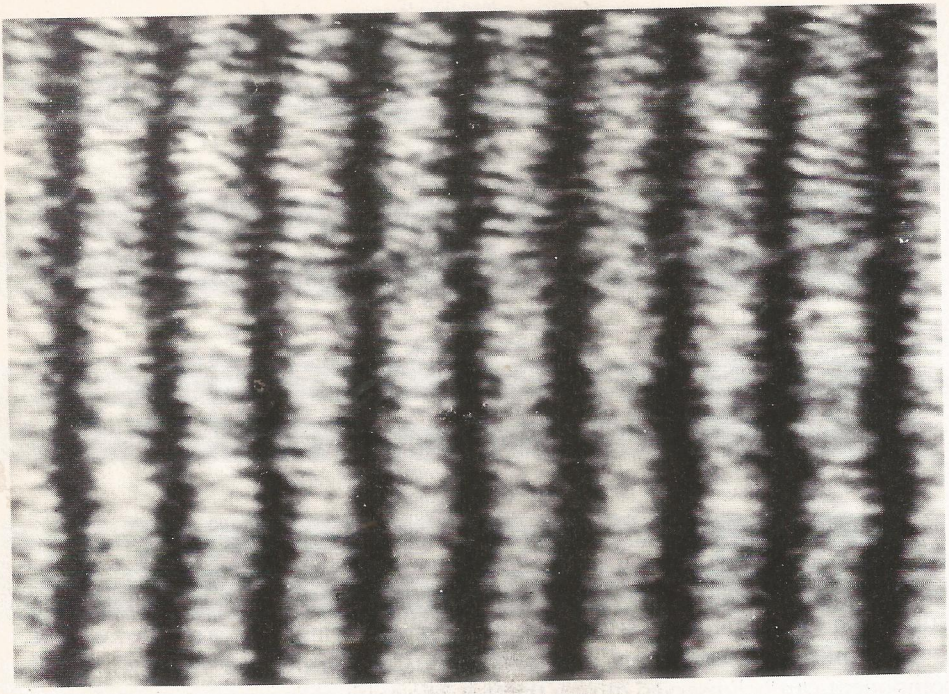

**Figure 5.9** Interference fringe pattern produced by reflected light from two V-shaped grooves. (*Courtesy of W. N. Sharpe, Jr.*)

As the light is reflected from the sides of the V grooves, two different interference patterns are formed, as indicated in Fig. 5.10. In an actual experimental situation, the fringe patterns are observed on screens located approximately 8 in (200 mm) from the grooves.

The intensity in the interference pattern goes to zero and a dark fringe is produced whenever $\beta = n\pi$, with $n = 1, 2, 3, \ldots$, or when $\phi = (m + \frac{1}{2})\pi$, with $m = 0, 1, 2, \ldots$. When the specimen is strained, both the distance $d$ between

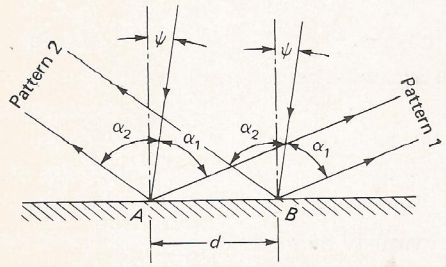


**Figure 5.10** Schematic diagram showing the light rays which form the two interference patterns.

grooves and the width $b$ of the grooves change. These effects produce shifts in the fringes of the two interference patterns which can be related to the average strain between the two grooves. The proof is beyond the scope of this presentation; however, it is shown in Ref. 10 that

$$\epsilon = \frac{(\Delta N_1 - \Delta N_2)\lambda}{2d \sin \alpha} \tag{5.11}$$

where $\Delta N_1$ and $\Delta N_2$ are the changes in fringe order in the two patterns produced by the strain and $\alpha$ is the angle between the incident light beam and the diffracted rays which produce the interference pattern.

The interferometric strain gage offers a method for measuring strain without actual use of a gage, thus eliminating any reinforcing effects or bonding difficulties. Since no contact is made, the method can be employed on rotating parts or in hostile environments. Again temperature compensation is automatic, and the method can be employed at very high temperatures.

## C. Electrical Strain Gages

During the past 30 years, electrical strain gages have become so widely accepted that they now dominate the entire strain-gage field except for a few special applications. The most important electrical strain gage is the resistance type, which will be covered in much greater detail in subsequent chapters. Two less commonly employed electrical strain gages, the capacitance type and the inductance type, will be introduced in this section. Although these gages have limited use in conventional stress analysis, they are often employed in transducer applications and on occasion find special application in measuring strain.

**The capacitance strain gage [11]** The capacitance of the parallel-plate capacitor illustrated in Fig. 5.11 can be computed from the relation

$$C = \begin{cases} 0.225 \dfrac{kA}{h} & \dfrac{A}{h} \text{ in inches} \\ 8.86 \times 10^{-3} \dfrac{kA}{h} & \dfrac{A}{h} \text{ in millimeters} \end{cases} \tag{5.12}$$

where $C$ = capacitance, pF
$k$ = dielectric constant of the medium between two plates
$A$ = cross-sectional area of the plates
$h$ = distance between two parallel plates

The flat-plate capacitor can be employed as a strain or displacement gage in one of three possible ways: (1) by changing the gap $h$ between the plates; (2) by moving one plate in a transverse direction with respect to the other, thereby changing the area $A$ between the two plates; and (3) by moving a body with a dielectric constant higher than air between the two plates.

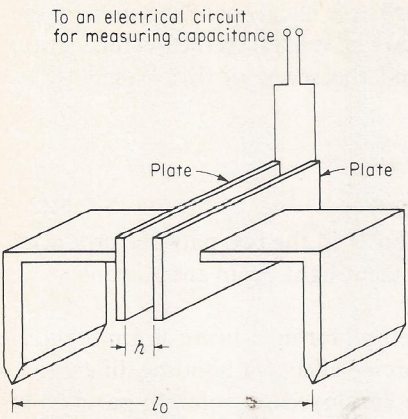


**Figure 5.11** Schematic illustration of a capacitor strain gage with a variable air gap.

A capacitor-type strain gage with a variable air gap is shown schematically in Fig. 5.11. The change in capacitance for a small change in the air gap $h$ can be obtained by differentiating Eq. (5.12) with respect to $h$ to obtain

$$\frac{dC}{dh} = 0.225kA\left(-\frac{1}{h^2}\right) = -\frac{C}{h} \tag{5.13}$$

When the gage illustrated in Fig. 5.11 is mounted to a specimen which in turn is loaded, the gage length will change by an amount $\Delta l$ and the air gap $h$ will change by $\Delta h = \Delta l$. Hence, the strain $\epsilon$ produces a change in capacitance $\Delta C$ which is given by Eq. (5.13) as

$$\epsilon = \frac{\Delta l}{l_0} = \frac{\Delta h}{l_0} = -\frac{h}{l_0}\frac{\Delta C}{C}$$

or

$$\frac{\Delta C}{C} = -\frac{l_0}{h}\epsilon \tag{5.14}$$

For a capacitor gage with $l_0 = 1$ in (25 mm), $h = 0.010$ in (0.25 mm), and $\epsilon = 1$ $\mu$in/in ($\mu$m/m), the value obtained for $\Delta C/C$ is $10^{-4}$. Electric circuits (a DeSauty ac bridge) can be employed to accurately measure capacitance changes as small as $\Delta C = C \times 10^{-4}$ for both static applications and low-frequency dynamic applications. Thus, the sensitivity and accuracy of the capacitor gage are quite sufficient for application to the general problem of determining strain distributions. The primary disadvantage of the capacitor gage is its relatively large size and its mechanical attachment through knife-edges. The application of the capacitor principle to other transducer systems, however, does show promise since it can be employed at elevated temperatures and the system involves very low operating forces.

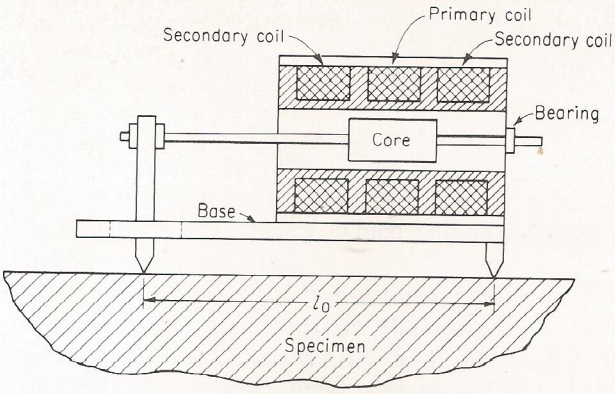


**Figure 5.12** Schematic illustration of a linear differential transformer employed as a strain transducer.

**The inductance strain gage** [12–13] Of the many types of inductance measuring systems which could be employed to measure strain, the differential-transformer system will be considered here. The linear differential transformer is an excellent device for converting mechanical displacement into an electrical signal. It can be employed in a large variety of transducers, including strain, displacement, pressure, acceleration, force, and temperature. A schematic illustration of a linear differential transformer employed as a strain-gage transducer is shown in Fig. 5.12. Mechanical knife-edges are displaced over the gage length by the strain induced in the specimen. This displacement is transmitted to the core, which moves relative to the coils, and an electrical output is produced across the coils.

A linear differential transformer has three coils, a primary coil and two secondary coils on either side of the primary. A core of magnetic material supported on a shaft of nonmagnetic material is positioned in the center of the coils, as shown in the circuit drawing in Fig. 5.13. As the core moves within the coils, it varies the mutual inductance between the primary and each secondary winding, with one secondary becoming more tightly coupled to the primary and the other secondary becoming more loosely coupled. The two secondary coils are wired in series opposition, and consequently the output voltage $E_0$ is the difference between the voltages developed in each secondary, that is, $E_0 = E_1 - E_2$. In a symmetrically constructed transformer a null output should occur when the core is at the center

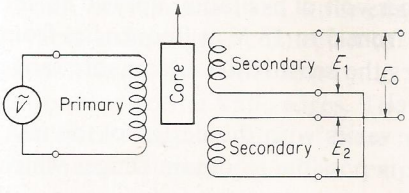


**Figure 5.13** Schematic diagram of the linear-differential-transformer circuit.

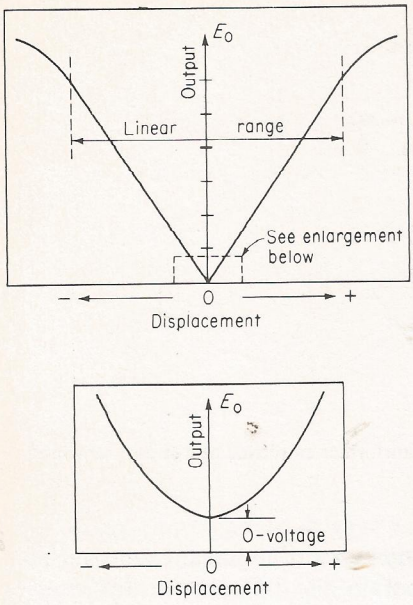


**Figure 5.14** Output voltage as a function of core position in a linear differential transformer.

point between the two secondary coils. Movement of the core in one direction off the null position will induce an unbalance in $E_1$ and $E_2$, and some net $E_0$ will be indicated. Displacement in the opposite direction will also produce an unbalance, with a resulting $E_0$ which is 180° out of phase with the first output. If the direction of the displacement must be known, the phase angle must be determined.

The above description refers to an ideal differential transformer in which the three coils are purely inductive and perfectly symmetrical, thus giving a perfect null voltage when the core is in the zero position. In reality, the differential transformer is not perfect and the output voltage goes to a minimum rather than a null at the zero position of the core. The output voltage for a typical differential transformer as a function of core position is given in Fig. 5.14.

The factor which is most detrimental to the formation of the null voltage is the capacitive coupling between the primary and secondary coils. This capacitive coupling will not produce opposing voltages across the two windings; hence $E_0$ will not go to null even when the inductively coupled voltages cancel out. The zero voltage is normally less than 1 percent of the maximum voltage; and unless extreme sensitivities are required, the error it induces is quite small.

The sensitivity of commercial differential transformers is of the order of 0.5 to 4 V/in (0.02 to 0.16 V/mm) of displacement per volt of excitation applied to the primary coil. The primary-coil voltage varies from 5 to 18 V at frequencies from 60 Hz to 2.4 kHz. At rated excitation voltages the sensitivities obtainable range from 4 to 65 V/in (0.16 to 2.6 V/mm) of travel.

The range of the differential transformer varies with the design of the unit. With commercially available transformers it is possible to obtain ranges which

vary from 0.020 to 2 in (0.5 to 50 mm). The greater the range of a particular transformer, the lower the sensitivity.

The errors of the linear differential transformer amount, in general, to about 0.5 percent of the maximum linear output. The deviation from linearity of the commercial units is also of the order 0.5 percent of the specified range. The dynamic response is limited by the mass of the core and supporting mechanical assembly. It is also limited electrically by the frequency of the applied ac voltage. This is a carrier frequency, which should be at least 10 times the maximum frequency being measured.

The linear differential transformer requires a very small driving force (a fraction of a gram) to move the core. The operation of the differential transformer can be severely affected, however, by the presence of metal masses or by stray magnetic fields. A magnetic shield is employed around the coil holder to minimize these effects.

In recent years the linear differential transformer has been supplied with a dc to ac power source and with a demodulator to condition the output voltage. When packaged as a single unit, the device is known as a DCDT. It is small, rugged, and extremely useful in the laboratory. It can be used for many applications since it can be powered with an ordinary 6-V dry cell and can be read out on a digital multimeter. Both these items are readily available in most laboratories. The use of the linear differential transformer or the DCDT for strain-gage applications has been limited because of the mechanical-attachment problem; however, it is one of the best displacement transducers available for general laboratory use.

## D. Acoustical Strain Gages [14–16]

Acoustical strain gages have been employed in a variety of forms in several countries since the late 1920s. To date they have been largely supplemented by the electrical-resistance strain gage. However, they are unique among all forms of strain gages in view of their long-term stability and freedom from drift over extended time periods. The acoustical gage described here, due to R. S. Jerrett, was developed in 1944. The strain-measuring system is based on the use of two acoustic gages referenced as a test gage and a reference gage. The significant parts of a gage are shown schematically in Fig. 5.15.

In the figure it can be seen that the gage has the commonly employed knife-edge mounting provision. One knife-edge is mounted to the main body, while the other knife-edge is mounted in a bearing suspension and is free to elongate with the specimen. The gage length $l_0$ is 3 in (76 mm). One end of a steel wire is attached to the movable knife-edge while the other end of the wire passes through a small hole in the fixed knife-edge and is attached to a tension screw. The movable knife-edge is connected to a second tension screw by a leaf spring. This design permits the initial tension in the wire to be applied without the transmission of load to the knife-edges. The wire passes between the pole pieces of two small electromagnets. One of these magnets is used to keep the wire vibrating at its natural frequency; the other is employed to pick up the frequency of the system.

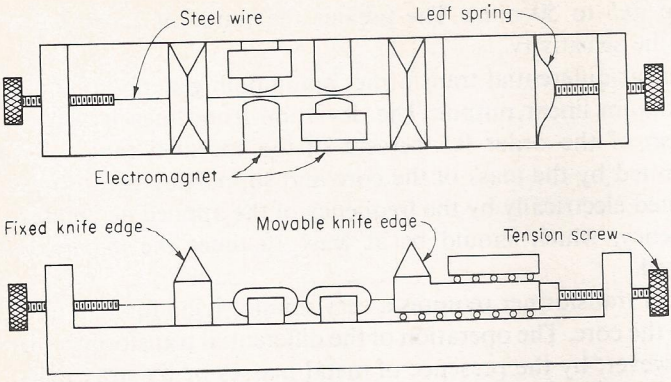


**Figure 5.15** Schematic drawing showing the operation of the Jerrett acoustical strain gage.

Electrically both magnets operate together in that the signal from the pickup magnet is amplified and fed back into the driving magnet to keep the string excited in its natural frequency.

The reference gage is very similar to the test gage except that the knife-edges are removed and a micrometer is used to tension the wire. A helical spring is employed in series with the wire to give larger rotations of the micrometer head for small changes of stress in the wire.

To operate the system, the test gage is mounted and adjusted and the reference gage is placed near it to attempt to compensate temperature effects. Both the gages are energized, and each wire will emit a musical note. If the frequency of vibrations from the two gages is not the same, beats will occur. The micrometer setting is varied on the reference gage until the beat frequency decreases to zero. The reading of the micrometer is then taken and the strain is applied to the test gage. The change in tension in the wire of the test gage produces a change in frequencies, and it is necessary to adjust the reference gage until the beats are eliminated. This new micrometer reading is proportional to the strain.

If the test gage is located in a remote position and the beat signals from the test and reference gages cannot be developed, it is possible to balance the two gages by using an oscilloscope. The voltage output from the pickup coils of each gage are displayed while operating the oscilloscope in the $xy$ mode. The resulting Lissajous figure provides the readout which permits adjustment of the reference gage to the frequency of the test gage.

The natural frequency of a wire held between two fixed points is given by

$$f = \frac{1}{2L}\sqrt{\frac{g\sigma}{w}} \tag{5.15}$$

where $L$ = length of wire between supports
$g$ = gravitational constant
$\sigma$ = stress in wire
$w$ = density of wire material
$f$ = frequency

In terms of strain in the wire the frequency is governed by the following equation, which comes directly from Eq. (5.15):

$$f = \frac{1}{2L}\sqrt{\frac{gE\epsilon}{w}} \tag{5.16}$$

where $E$ is the modulus of elasticity.

The sensitivity of this instrument is very high, with possible determinations of displacements of the order of 0.1 $\mu$in (2.5 nm). The range is limited, in general, to about one-thousandth of the wire length before over- or understressing of the sensing wire becomes critical. The gage is temperature-sensitive unless the thermal coefficients of expansion of the base and wire are closely matched over the temperature range encountered during a test. Finally, the force required to drive the transducer is relatively large, and it should therefore not be employed in systems where the large driving force will be detrimental.

## 5.4 MOIRÉ METHOD OF STRAIN ANALYSIS [17, 18]

Discussed in the preceding section were various types of strain gages which permit the determination of an average normal strain along a line segment of length $l_0$ on the surface of a specimen. The use of these gages, in effect, gives the value of one normal component of strain at one point on the surface of the specimen. A complete determination of the strain field entails the application of a large number of these gages so that $\epsilon_{xx}$, $\epsilon_{yy}$, $\gamma_{xy}$ can be evaluated over the major portion of the surface. The point-per-point method of evaluation of each of the three cartesian components of strain is a time-consuming and expensive approach to a complete evaluation of a general strain field.

The moiré method of strain analysis, which permits a whole-field examination of the strain in a simple and direct fashion, has been developed to a point where it can be employed in certain problems where the displacements are relatively large. A complete treatment of the moiré method is presented in Chap. 12.

## 5.5 GRID METHOD OF STRAIN ANALYSIS [19–25]

The grid method of strain analysis is one of the oldest techniques known to experimental stress analysis. The method requires placement of a grid (a series of well-defined parallel lines) on the surface of the specimen. Next, the grid is carefully photographed before and after loading the specimen to obtain negatives which will show the distortion of the grid. Measurements of the distance between the grid lines before and after deformation give lengths $l_i$ and $l_f$ respectively. These lengths may be interpreted in terms of strain in several different ways:

Lagrangian strain:
$$\epsilon = \frac{l_f - l_i}{l_i} \tag{5.17}$$

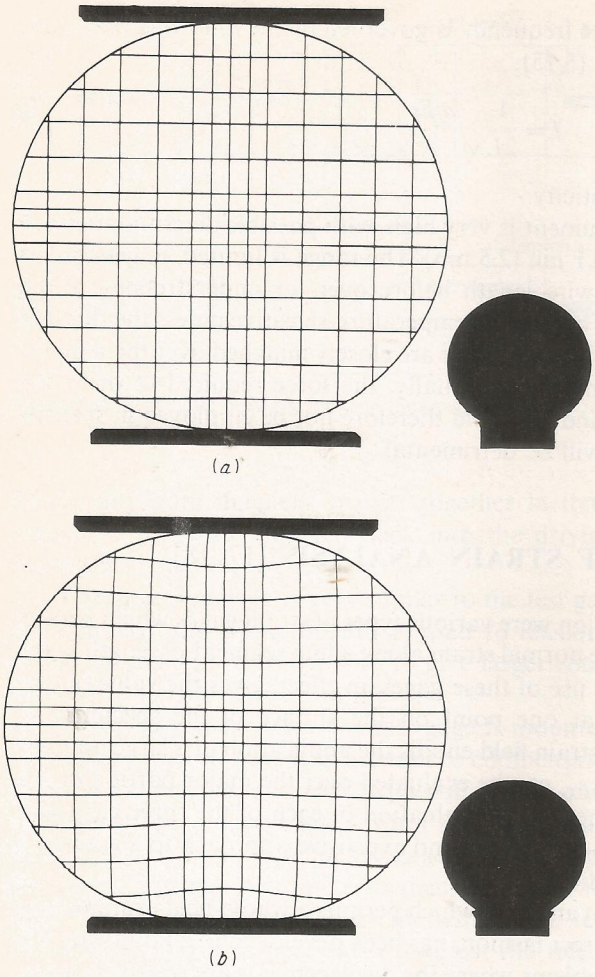


**Figure 5.16** An embedded rubber-thread grid in a transparent rubber model of a circular disk under diametral compression: (*a*) before deformation; (*b*) after deformation.

Eulerian strain:
$$\epsilon = \frac{l_f - l_i}{l_f} \tag{5.18}$$

Natural strain:
$$\epsilon = \ln \frac{l_f}{l_i} \tag{5.19}$$

The exact form used to determine the strain will depend upon the purpose of the analysis and the amount of deformation experienced by the model.

If the grid consists of two series of orthogonal parallel lines over the entire surface of the specimen (see Fig. 5.16), the grid method will give strain components over the entire field. The strain component $\epsilon_{xx}$ in the horizontal direction is obtained by comparing the distances between the vertical grid lines before and after deformation. The vertical or $\epsilon_{yy}$ component of strain can be obtained from

the horizontal array of grid lines, and the $\epsilon_{45^\circ}$ component of strain can be obtained from measurements across the diagonals if the orthogonal grid array is square.

In general, two main difficulties are associated with the utilization of the grid method for measuring strain. First, the strains being measured are usually quite small, and in most instances the displacement readings cannot be made with sufficient precision to keep the accuracy of the strain determinations within reasonable limits. Also, the definition of the grid lines on the negatives is usually poor when magnified, so that appreciable errors are introduced in the displacement readings.

In order to effectively employ the grid method and avoid these two difficulties, the deformations applied to the model must be large enough to impose strain levels of the order of 5 percent. Usually model deformations this large are to be avoided in an elastic stress analysis; hence other experimental methods such as the moiré method or electrical-resistance strain gages are preferred. However, when large deformations are associated with the stress-analysis problem, e.g., plastic deformations or deformations in rubberlike materials, the grid method is one of the most effective methods known. In fact, if the strains exceed 20 to 30 percent, the range of the commonly employed strain gages is exceeded, and only the moiré method or the grid method is adequate for measuring these large strains.

Usually the most critical step in employing the grid method involves the placement of the grid array on the model being investigated. Methods used for this purpose include hand scratching, ink ruling, machine scribing, and photoprinting. More recently, a technique for embedding a rubber-thread grid in a transparent urethane rubber model has been developed by Durelli and Riley which has distinct advantages. With this technique, the grid consists of thin, extruded rubber threads which are stretched to reduce their original diameter of 0.008 in (0.2 mm) to about 0.004 in (0.1 mm). Instead of being cemented to the specimen after it is machined, the grid is threaded in the appropriate array through the sides of a plate mold, and the transparent rubber is cast about it. In this manner, the grid can be located at any desired position in the plane of the model. Upon curing, the sheet of transparent rubber contains the embedded grid and can be machined to the model geometry. This model can then be subjected to load, and both grid and photoelastic data can be recorded simultaneously. These data, together with the elastic constants of the rubber, are sufficient to provide a complete solution of two-dimensional stress problems.

### The Replica Technique [25]

A modification of the grid method for determining static strains which eliminates the requirement for accurate placement of a grid array on the specimen has been developed by Hickson. With this method, a family of parallel scratches of uneven spacing and thickness is applied to a polished region of a specimen by drawing fine abrasive paper along the edge of a template. Lines equivalent to those produced by the best engraving techniques are frequently present in such a scratch

pattern. A second pattern, applied perpendicular to the first, produces the rectangular array of lines required for grid analyses of deformation and strain. A coarse pattern of broad reference lines is scribed over the scratch pattern to serve as datum lines and to help identify specific scratch lines being used for measurements.

Since it is extremely difficult to make precise measurements of displacement with the specimen under load, a replica technique is used to record the scratch patterns before and after loading. The replicas are made by using a thin film of fusible alloy on a stiffening platen. The alloy is capable of reproducing the finest detail in the scratch pattern. The platen serves to provide dimensional stability and temperature compensation if it is made of the same material as the specimen. Such replicas have been shown to be accurate to at least 40 $\mu$in (1 $\mu$m).

Displacement measurements are made by comparing a pair of replicas, taken before and after loading, with a microscope fitted with a micrometer eyepiece. The two replicas are mounted in a holder which permits the two scratch patterns to be viewed alternately in the same part of the microscope field. The identification of lines being used for strain determinations is simplified by use of the reference grid and the random nature of the lines in the scratch pattern. Accurate measurement of displacements between the high-quality lines in the patterns permits strain determinations in situations not possible by other means, e.g., near a crack or in two plates after joining by welding.

## EXERCISES

**5.1** The stress distribution in a thin wide plate with a central circular hole is given by Eq. (3.46) when the plate is subjected to a uniaxial tensile or compressive load. Determine the error made in the determination of the maximum stress $\sigma_{max}$ on the boundary of the hole if a strain gage having a gage length $l_0 = 6$ mm is used. The diameter of the hole in the plate is 25 mm. $E = 200$ GPa, $\nu = 0.30$.)

**5.2** Determine the error associated with measurements of $\epsilon_{yy}$ along the longitudinal axis of the plate of Exercise 5.1 if gages with $l_0/a = \frac{1}{4}$ are located at $y/a = 1.5$, 2.0, and 3.0.

**5.3** Determine the error associated with measurements of $\epsilon_{yy}$ along the transverse axis of the plate of Exercise 5.1 if gages with a width $w_0/a = \frac{1}{8}$ are located at $x/a = 1.5$, 2.0, and 3.0.

**5.4** For the plate of Exercise 5.1, determine the error associated with measurements of $\epsilon_{yy}$ along the transverse axis of the plate due to both gage width and gage length. Take $w_0/a = \frac{1}{8}$ and $l_0/a = \frac{1}{4}$ and consider gages located at $x/a = 1.5$, 2.0, and 3.0.

**5.5** Consider a strain field given by the expression $\epsilon_{xx} = b \sin(\pi x/a)$. Determine the error made in the measurement of $\epsilon_{xx}$ at $x = 0$, $a/4$, and $a/2$ when $l_0/a = \frac{1}{2}$, $\frac{1}{4}$, and $\frac{1}{10}$.

**5.6** Consider a strain field given by the expression $\epsilon_{xx} = b + b \sin(\pi x/a)$. Determine the error made in the measurement of $\epsilon_{xx}$ at $x = a/2$ when $l_0/a = \frac{1}{4}$. Compare with the results of Exercise 5.5.

**5.7** Consider a strain field given by the expression $\epsilon_{xx} = b + bx + b \sin(\pi x/a)$. Determine the error made in the measurement of $\epsilon_{xx}$ at $x = a/2$ when $l_0/a = \frac{1}{4}$. Compare with the results from Exercises 5.5 and 5.6. What is the effect of adding constant and linear contributions to the strain field on the overall error?

**5.8** A model of a Huggenberger type of strain gage is to be constructed for a classroom demonstration. The following dimensions have been suggested: $r_1 = 50$ mm, $r_2 = 500$ mm, $w_1 = 100$ mm, and $w_2 = 500$ mm. Determine (*a*) the magnification factor for the demonstration model and (*b*) the arc